

Article

Bright, Dark, and Rogue Wave Soliton Solutions of the Quadratic Nonlinear Klein–Gordon Equation

Alrazi Abdeljabbar ^{1,*} , Harun-Or Roshid ² and Abdullah Aldurayhim ³¹ Department of Mathematics, Khalifa University, Abu Dhabi P.O. Box 127788, United Arab Emirates² Department of Mathematics, Pabna University of Science and Technology, Pabna 6600, Bangladesh; harunoroshidmd@gmail.com or harun_math@pust.ac.bd³ Department of Mathematics, College of Science and Humanities in Alkharj, Prince Sattam bin Abdulaziz University, Alkharj 11942, Saudi Arabia; am.aldurayhim@psau.edu.sa

* Correspondence: alrazi.abdeljabbar@ku.ac.ae

Abstract: This article reflects on the Klein–Gordon model, which frequently arises in the fields of solid-state physics and quantum field theories. We analytically delve into solitons and composite rogue-type wave propagation solutions of the model via the generalized Kudryashov and the extended Sinh Gordon expansion approaches. We obtain a class of analytically exact solutions in the forms of exponential and hyperbolic functions involving some arbitrary parameters with the help of Maple, which included comparing symmetric and non-symmetric solutions with other methods. After analyzing the dynamical behaviors, we caught distinct conditions on the accessible parameters of the solutions for the model. By applying conditions to the existing parameters, we obtained various types of rogue waves, bright and dark bells, combing bright–dark, combined dark–bright bells, kink and anti-kink solitons, and multi-soliton solutions. The nature of the solitons is geometrically explained for particular choices of the arbitrary parameters. It is indicated that the nonlinear rogue-type wave packets are restricted in two dimensions that characterized the rogue-type wave envelopes.

Keywords: the Klein–Gordon; the generalized Kudryashov scheme; the extended Sinh Gordon expansion scheme; solid-state physics; rogue wave; bright bell; dark bell profile



Citation: Abdeljabbar, A.; Roshid, H.-O.; Aldurayhim, A. Bright, Dark, and Rogue Wave Soliton Solutions of the Quadratic Nonlinear Klein–Gordon Equation. *Symmetry* **2022**, *14*, 1223. <https://doi.org/10.3390/sym14061223>

Academic Editor: Kazuharu Bamba

Received: 28 April 2022

Accepted: 2 June 2022

Published: 13 June 2022

Publisher's Note: MDPI stays neutral with regard to jurisdictional claims in published maps and institutional affiliations.



Copyright: © 2022 by the authors. Licensee MDPI, Basel, Switzerland. This article is an open access article distributed under the terms and conditions of the Creative Commons Attribution (CC BY) license (<https://creativecommons.org/licenses/by/4.0/>).

1. Introduction

The exciting tripping subsistence of rogue waves has been forecast and detected in a lot of physical scenarios, extending from oceanography [1] to hydrodynamics [2], as well as nonlinear optical systems [3,4] to plasma state physics [5,6]. The hypothetical inquiries of physical resonance phenomena through nonlinear evolution equations are becoming dictatorial day by day. Because there are more vigorous intricate phenomena in miscellaneous grounds, complex nonlinear scientific and engineering problems can be decorated by exact explicit solutions of nonlinear models. Much effort has been devoted to constructing the analytical solutions for the nonlinear evolution equation (NLEEs) [1–25].

In contrast with tsunamis and storms allied with typhoons that may possibly be able to be predicted hours in advance, rogue-type surfs are abruptly visible from nowhere and become invisible without trace [3]. They have also caught the interest of the extensive technical community [4–8], and been detected in optical fiber communications [4], in plasmas [5,6], in capillaries [7], and quantum fields [8]. Recently, in the nonlinear field, rogue wave (RW), lump solutions, and breather waves have received more interest and devotion [9–16]. Deformed defective soliton solutions were established and discussed in the Refs. [17–20]. The applications and behaviors of various types of solitons in Bose–Einstein condensates were discussed by energetic researchers [21–24]. Besides this, various effective approaches have been established to derive complex nonlinear models to extract soliton and multi-soliton solutions in the literature [25–27]. Very recently, kink–anti-kink scattering and interactions were discussed in the Refs. [28,29] in detail.

In this effort, our aim is to derive various types of rogue, bright bell, and dark bell envelope solutions of the well-known nonlinear Klein–Gordon model (KGM) [30–34],

$$U_{tt} - \alpha^2 U_{xx} + \beta U - \gamma U^2 = 0 \quad (1)$$

by the advantage of the generalized Kudryashov method (GKM) [35–41] and the extended Sinh Gordon expansion (EShGE) techniques [42]. In Equation (1), α is the second-order spatial dispersion and γ is the coefficient of quadratic nonlinearity. From the analysis of each term and traveling wave variable $\xi = kx - \omega t$, it is clear that Equation (1) is Lorentz-invariant. The KGM (1) arises in different numerous scientific applications in relativistic quantum fields, such as the transmission of disruption and the Bloch wall activity of magnets in crystals, magnetic flux on a Josephson line, a “splay wave” through a membrane, and so on [30,34]. In fact, this model is the opening relativistic field equation amid the quantum workings of wave profiles due to zero spin. Several appreciated and confident techniques have been proposed to extract precise solutions of the quadratic nonlinear KGM [30–34]. The application of these methods has been restricted to obtaining periodic and soliton solutions. Here is a question of the possibility to obtain similar symmetric and non-symmetric periodic solitons and even rogue-type breather wave solutions for this model. Thus, we chose the well-known GKM [35–41] and the EShGE method [42] to determine distinct and more significant solutions that can construct better rogue and solitary waves than the other approaches [30–34].

The composition of the remainder of this article is as follows: In Section 2, we recall the summarization of the GKM and the EShGE. In Section 3, we demonstrate exact analytic solutions of the KGM with quadratic nonlinearity using the GKM and the EShGE method. Then, in Section 4, we present diverse rogue-type waves, bright bell-like, and dark bell-like profiles with 3-D and 2-D diagrams. Finally, we present a graphical illustration of the obtained solutions in the final section.

2. Methods

We briefly here discuss the two elegant methods, namely, the GKM and the EShGE method, to integrate any nonlinear evolution equations.

2.1. General Form of the GKM

In this part, we disclose the working route of the GKM, which was introduced by Kudryashov [35], broadly to pursue explicitly analytic solutions for any nonlinear models. Reflect a nonlinear model of the form,

$$Q(U, U_{xt}, U_{xxt}, U_{xx}, U_t, U_{tt}, \dots) = 0, \quad (2)$$

where $U(x, t)$ is an unrevealed function and Q includes various partial derivatives of $U(x, t)$ involving complex non-linearities.

Step 1: To switch the nonlinear partial differential Equation (2) into the ordinary differential equation (ODE), anyone can use the wave-transformation relation,

$$R(x, t) = R(\xi), \quad \xi = kx - \omega t, \quad (3)$$

where k, ω are the wave number and velocity, respectively. Therefore, inserting Equation (3) into the Equation (2), we reach a corresponding ODE as

$$Q_1(U_\xi, UU_\xi, U_{\xi\xi}, UU_{\xi\xi}, U_{\xi\xi\xi}, \dots) = 0. \quad (4)$$

If Equation (4) is integrable, then we integrate Equation (4) as many times as necessary considering every integral constant as zero.

Step 2: Deeming that the trial solution has the general structure as a polynomial function of $F(\xi)$:

$$U(\xi) = \frac{\sum_{i=0}^N a_i (F(\xi))^i}{\sum_{j=0}^M b_j (F(\xi))^j}, \quad (5)$$

where $a_i, b_j, \omega, k; i = 0, \dots, m, j = 0, \dots, n$ are unfamiliar and will be evaluated afterward, while $a_N \neq 0, b_M \neq 0$ together, where N and M are the positive integer, whose particular values can be derived by balancing the power of nonlinear and height derivative terms.

We have a condition of $F(\xi)$ satisfying the Riccati equation,

$$F'(\xi) = F^2(\xi) - F(\xi), \quad (6)$$

with a solution $F(\xi) = (1 + h e^{\xi})^{-1}$.

Step 3: Merging Equation (5) and Equation (4) with the ODE (6), and assembling identical order of $F(\xi)$ collectively, we present an algebraic polynomial for $F(\xi)$. Setting each of the coefficients of $F(\xi)$ equal to zero acquiesces some algebraic systems of $a_i, b_j, \omega, k; i = 0, \dots, m, j = 0, \dots, n$. Solving the unknowns and setting them into Equation (5), we reach the analytic wave solutions of the model Equation (2).

2.2. The EShGE Method

In this part, we disclose the working route of the EShGE method [42] briefly to pursue the explicit and analytical solutions of any nonlinear models. We convert the NLEEs (2) into ODE (4) in a similar way as in the previous method. Then, we carry the trial solution as

$$H(F) = a_0 + \sum_{\ell=1}^n \cosh^{\ell-1} F (b_{\ell} \sinh F + a_{\ell} \cosh F). \quad (7)$$

The function F satisfies the ODE $F' = \sinh(F)$ extracted from the Sinh Gordon model $u_{xt} = \mu \sinh u$ [25] and gives the solutions,

$$\sinh F = \pm i \sec h \xi \text{ or } \sinh F = \pm \csc h \xi \text{ with } i = \sqrt{-1} \quad (8)$$

$$\cosh F = \pm \tanh \xi \text{ or } \cosh F = \pm \coth \xi \quad (9)$$

Now, differentiating (7) twice along with $F' = \sinh(F)$ and inserting these into the ODE (4) yields a set of unknown equations in a_0, a_{ℓ}, b_{ℓ} . Solving and inserting the solutions of the system into (7) with (8) and (9) gives the return results.

2.3. Multi-Soliton via Burgers' Model Scheme

In this part, we disclose the working route to derive a multi-kink wave solution using the Burgers' model

$$B_t - 2BB_x - B_{xx} = 0. \quad (10)$$

The multi-soliton solution of (10) is

$$B = \frac{\sum_{j=1}^n k_j e^{k_j x - \omega_j t}}{1 + \sum_{j=1}^n e^{k_j x - \omega_j t}}, \quad (11)$$

where k_j, ω_j are constants and n is a positive integer number. Treat the traveling variable $\xi = kx - \omega t$, so that $B(\xi) = B(x, t)$ with the dispersion relation $k_j = -\omega_j^2$ and convert the Burgers' equation into

$$B' = B - B^2/k. \quad (12)$$

Using this equation as an auxiliary multi-soliton solution of $(1 + 1) - D$ models is possible.

3. Extract Solutions through the Schemes

In these parts, we focus on presenting the applications of the GKM and the EShGE to the KGM for extracting wave solutions of the above-mentioned Klein–Gordon (KG) model.

3.1. Application of the GKM to the KGM

In this part, we explore a reliable treatment of the KGM with the help of the GKM. We first implement the GKM in the quadratic nonlinear $(1 + 1)$ -dimensional KGM (1). Utilizing the wave transformation relation Equation (3), we revamp Equation (1) into the ODE:

$$(\omega^2 - \alpha^2 k^2)H'' + \beta H - \gamma H^2 = 0. \tag{13}$$

The terms H'' and H^2 provide us the balance number of (10) as $N = M + 2$.

For the unit value of M , we reach the trial solution of Equation (5), taking the form as:

$$H(\xi) = \frac{a_0 + a_1 F(\xi) + a_2 (F(\xi))^2 + a_3 (F(\xi))^3}{b_0 + b_1 F(\xi)}. \tag{14}$$

We now differentiate (14) with respect to ξ along with (6), and then insert U, U', U'' into (13), giving an equation. Equating the coefficients of $F^l(\xi)$ from the required equation equal to zero yields:

$$\begin{aligned} (F(\xi))^7 : & \gamma a_3^2 b_1 - 6\omega^2 a_3 b_1^2 + 6\alpha^2 k^2 a_3 b_1^2 = 0, \\ (F(\xi))^6 : & -10\alpha^2 k^2 a_3 b_1^2 + 10\omega^2 a_3 b_1^2 + \gamma a_3^2 b_0 + 2\alpha^2 k^2 a_2 b_1^2 - 16\omega^2 a_3 b_0 b_1 \\ & + 2\gamma a_2 a_3 b_1 - 2\omega^2 a_2 b_1^2 + 16\alpha^2 k^2 a_3 b_0 b_1 = 0, \\ (F(\xi))^5 : & -16\omega^2 a_2 b_0 b_1 - 4\omega^2 a_3 b_1^2 + 2\gamma a_2 a_3 b_0 + \gamma a_2^2 b_1 - 3\alpha^2 k^2 a_2 b_1^2 \\ & + 6\alpha^2 k^2 a_2 b_0 b_1 - 27\alpha^2 k^2 a_3 b_0 b_1 + 2\gamma a_1 a_3 b_1 - \beta a_3 b_1^2 + 4\alpha^2 k^2 a_3 b_1^2 \\ & + 12\alpha^2 k^2 a_2 b_0^2 + 27\omega^2 a_3 b_0 b_1 - 12\omega^2 a_3 b_0^2 + 3\omega^2 a_2 b_1^2 = 0, \\ (F(\xi))^4 : & -\omega^2 a_2 b_1^2 - 11\omega^2 a_3 b_0 b_1 + \gamma a_2^2 b_0 + 2\gamma a_0 a_3 b_1 + 2\gamma a_1 a_3 b_0 - 6\omega^2 a_2 b_0^2 \\ & - 21\alpha^2 k^2 a_3 b_0^2 + 21\omega^2 a_3 b_0^2 + \alpha^2 k^2 a_2 b_1^2 - \beta a_2 b_1^2 - 2\beta a_3 b_0 b_1 - 9\alpha^2 k^2 a_2 b_0 b_1 \\ & + 2\gamma a_1 a_2 b_1 + 11\alpha^2 k^2 a_3 b_0 b_1 + 9\omega^2 a_2 b_0 b_1 + 6\alpha^2 k^2 a_2 b_0^2 = 0, \\ (F(\xi))^3 : & -\alpha^2 k^2 a_0 b_1^2 + 2\alpha^2 k^2 a_1 b_0^2 + 2\gamma a_0 a_3 b_0 + 10\omega^2 a_2 b_0^2 - \omega^2 a_1 b_0 b_1 + 2\gamma a_1 a_2 b_0 \\ & + 9\alpha^2 k^2 a_3 b_0^2 - 3\omega^2 a_2 b_0 b_1 + \alpha^2 k^2 a_1 b_0 b_1 - 9\omega^2 a_3 b_0^2 + 2\gamma a_0 a_2 b_1 + 3\alpha^2 k^2 a_2 b_0 b_1 \\ & - 2\beta a_2 b_0 b_1 + 2\omega^2 b_1 a_0 b_0 - \beta a_3 b_0^2 + \gamma a_1^2 b_1 - 2\alpha^2 k^2 b_1 a_0 b_0 + \omega^2 a_0 b_1^2 \\ & - 10\alpha^2 k^2 a_2 b_0^2 - \beta a_1 b_1^2 - 2\omega^2 a_1 b_0^2 = 0, \\ (F(\xi))^2 : & -3\alpha^2 k^2 a_1 b_0^2 - 2\beta a_1 b_0 b_1 + 4\alpha^2 k^2 a_2 b_0^2 - \alpha^2 k^2 a_1 b_0 b_1 - 3\omega^2 b_1 a_0 b_0 \\ & + 3\alpha^2 k^2 b_1 a_0 b_0 + \alpha^2 k^2 a_0 b_1^2 + \omega^2 a_1 b_0 b_1 + \gamma a_1^2 b_0 - \omega^2 a_0 b_1^2 - \beta a_0 b_1^2 \\ & + 3\omega^2 a_1 b_0^2 + 2\gamma a_0 a_1 b_1 + 2\gamma a_0 a_2 b_0 - \beta a_2 b_0^2 - 4\omega a_2 b_0^2 = 0, \\ (F(\xi)) : & \omega^2 b_1 a_0 b_0 - 2\beta b_1 a_0 b_0 + \alpha^2 k^2 a_1 b_0^2 - \omega^2 a_1 b_0^2 - \alpha^2 k^2 b_1 a_0 b_0 \\ & + 2\gamma a_0 a_1 b_0 + \gamma a_0^2 b_1 - \beta a_1 b_0^2 = 0, \\ (F(\xi))^0 : & \gamma a_0^2 b_0 - \beta a_0 b_0^2 = 0. \end{aligned}$$

The above system of equations yields four classes of solutions:

Set01: $\omega = \sqrt{\alpha^2 k^2 + \beta}, a_0 = \frac{\beta b_0}{\gamma}, a_1 = -\frac{\beta(-b_1+6b_0)}{\gamma}, a_2 = -\frac{6\beta(-b_1+b_0)}{\gamma}, a_3 = \frac{6\beta b_1}{\gamma}$, where b_0, b_1, k are constants.

Then, inserting these values of Set01 into (14), progress the following solution

$$U(x, t) = \frac{\beta b_0(1 + he^\xi)^3 - \beta(-b_1 + 6b_0)(1 + he^\xi)^2 - 6\beta(-b_1 + b_0)(1 + he^\xi) + 6\beta b_1}{\gamma(1 + he^\xi)^2\{b_0(1 + he^\xi) + b_1\}}, \quad (15)$$

where $\xi = kx - \sqrt{\alpha^2 k^2 + \beta}t$, and $k, \alpha, \beta, \gamma, b_0$ and b_1 are arbitrary constants. The velocity of this wave solution is $\sqrt{\alpha^2 k^2 + \beta}/k$.

Set02: $k = k, \omega = \sqrt{\alpha^2 k^2 - \beta}, a_0 = \frac{6\beta b_0}{\gamma}, a_1 = \frac{6\beta b_0}{\gamma}, a_2 = -\frac{6\beta(-b_1 + b_0)}{\gamma}, a_3 = -\frac{6\beta b_1}{\gamma}, b_0 = b_0, b_1 = b_1$.

Inserting Set02 into (14) takes the following form

$$U(x, t) = \frac{6\beta b_0(1 + he^\xi)^3 + 6\beta b_0(1 + he^\xi)^2 - 6\beta(-b_1 + b_0)(1 + he^\xi) - 6\beta b_1}{\gamma\{b_0(1 + he^\xi) + b_1\}}, \quad (16)$$

where $\xi = kx - \sqrt{\alpha^2 k^2 - \beta}t$, and $k, \alpha, \beta, \gamma, b_0$ and b_1 are arbitrary constants. The velocity of this wave solution is $\sqrt{\alpha^2 k^2 - \beta}/k$.

Set03: $k = \frac{\sqrt{\omega^2 - \beta}}{\alpha}, a_0 = \frac{a_3}{6} + \frac{a_2}{6}, a_1 = -a_2 - \frac{5a_3}{6}, b_0 = \frac{\gamma(a_3 + a_2)}{6\beta}, b_1 = \frac{\gamma a_3}{6\beta}$, and ω, a_2, a_3 are arbitrary constants.

With Set03, Equation (14) becomes

$$U(x, t) = -\frac{(-h^2 e^{2\xi} + 4he^\xi - 1)\beta}{\gamma(he^\xi + 1)^2}, \quad (17)$$

where $\xi = \frac{\sqrt{\omega^2 - \beta}}{\alpha}x - \omega t$, and k, α, β, γ and h are arbitrary constants. The velocity of this wave solution is $\omega\alpha/\sqrt{\omega^2 - \beta}$.

Set04: $k = \frac{\sqrt{\omega^2 + \beta}}{\alpha}, a_0 = 0, a_1 = -a_3 - a_2, b_0 = \frac{\gamma(a_3 + a_2)}{-6\beta}, b_1 = -\frac{\gamma a_3}{6\beta}$, and ω, a_2, a_3 are arbitrary constants.

Inserting the values of the parameters into (14), we obtain the solution

$$U(x, t) = \frac{6he^\xi \beta}{\gamma(he^\xi + 1)^2}, \quad (18)$$

where $\xi = \frac{\sqrt{\omega^2 + \beta}}{\alpha}x - \omega t$, and k, α, β, γ and h are arbitrary constants. The velocity of this wave solution is $\omega\alpha/\sqrt{\omega^2 + \beta}$.

3.2. Application of the EShGE to the KGM

This part extracts the solutions of model (1) via the EShGE method. We know that the balance number of our model is $N = 2$. Thus, the trial solution of the EShGE technique reduces to

$$H(F) = a_0 + b_1 \sinh F + a_1 \cosh F + b_2 \sinh F \cosh F + a_2 \cosh^2 F. \quad (19)$$

Switching (19) and its second derivative with $F' = \sinh(F)$ into (13), and then gathering the polynomial as the coefficients of hyperbolic function, we have:

$$\begin{aligned} -6\alpha^2 k^2 b_2 - 2\gamma a_2 b_2 + 6\omega^2 b_2 &= 0, \\ -2\alpha^2 k^2 b_1 - 2\gamma a_1 b_2 - 2\gamma a_2 b_1 + 2\omega^2 b_1 &= 0, \\ 5\alpha^2 k^2 b_2 - 2\gamma a_0 b_2 - 2\gamma a_1 b_1 - 5\omega^2 b_2 + \beta b_2 &= 0, \\ \alpha^2 k^2 b_1 - 2\gamma a_0 b_1 - \omega^2 b_1 + \beta b_1 &= 0, \end{aligned}$$

$$\begin{aligned}
& -6\alpha^2 k^2 a_2 - \gamma a_2^2 - \gamma b_2^2 + 6\omega^2 a_2 = 0, \\
& -2\alpha^2 k^2 a_1 - 2\gamma a_1 a_2 - 2\gamma b_1 b_2 + 2\omega^2 a_1 = 0, \\
& 8\alpha^2 k^2 a_2 - 2\gamma a_0 a_2 - \gamma a_1^2 - \gamma b_1^2 + \gamma b_2^2 - 8\omega^2 a_2 + \beta a_2 = 0, \\
& 2\alpha^2 k^2 a_1 - 2\gamma a_0 a_1 + 2\gamma b_1 b_2 - 2\omega^2 a_1 + \beta a_1 = 0, \\
& -2\alpha^2 k^2 a_2 - \gamma a_0^2 + \gamma b_1^2 + 2\omega^2 a_2 + \beta a_0 = 0.
\end{aligned}$$

The system of equations provides us with six sets of solutions:

Set01: When $a_0 = \frac{3\beta}{2\gamma}$, $a_1 = 0$, $a_2 = -\frac{3\beta}{2\gamma}$, $b_1 = 0$, $b_2 = 0$, $\omega = \frac{1}{2}\sqrt{4\alpha^2 k^2 - \beta}$, the solutions become

$$H_1(\xi) = \frac{3\beta}{2\gamma} \pm \left(-\frac{3\beta}{2\gamma}\right) \tanh^2 \xi. \quad (20)$$

and

$$H_2(\xi) = \frac{3\beta}{2\gamma} \pm \left(-\frac{3\beta}{2\gamma}\right) \coth^2 \xi \quad (21)$$

where $\xi = kx - \frac{1}{2}\sqrt{4\alpha^2 k^2 - \beta}t$, and α, β, γ and k are free constants. The velocity of the wave solutions Equations (20) and (21) is $\sqrt{4\alpha^2 k^2 - \beta}/(2k)$.

Set02: When $a_0 = -\frac{\beta}{2\gamma}$, $a_1 = 0$, $a_2 = \frac{3\beta}{2\gamma}$, $b_1 = 0$, $b_2 = 0$, $\omega = \frac{1}{2}\sqrt{4\alpha^2 k^2 + \beta}$, the solutions become

$$H_3(\xi) = -\frac{\beta}{2\gamma} \pm \left(\frac{3\beta}{2\gamma}\right) \tanh^2 \xi \quad (22)$$

and

$$H_4(\xi) = -\frac{\beta}{2\gamma} \pm \left(\frac{3\beta}{2\gamma}\right) \coth^2 \xi \quad (23)$$

where $\xi = kx - \frac{1}{2}\sqrt{4\alpha^2 k^2 + \beta}t$, and α, β, γ and k are arbitrary constants. The velocity of the wave solutions Equations (22) and (23) is $\sqrt{4\alpha^2 k^2 + \beta}/(2k)$.

Set03: For $a_0 = -\frac{2\beta}{\gamma}$, $a_1 = 0$, $a_2 = b_2 = \frac{3\beta}{\gamma}$, $b_1 = 0$, $\omega = \sqrt{\alpha^2 k^2 + \beta}$, the solutions become

$$H_5(\xi) = -\frac{2\beta}{\gamma} \pm i \frac{3\beta}{\gamma} \tanh \xi \sec h \xi \pm \frac{3\beta}{\gamma} \tanh^2 \xi \quad (24)$$

and

$$H_6(\xi) = -\frac{2\beta}{\gamma} \pm \frac{3\beta}{\gamma} \coth \xi \operatorname{csch} \xi \pm \frac{3\beta}{\gamma} \coth^2 \xi \quad (25)$$

where $\xi = kx - \sqrt{\alpha^2 k^2 + \beta}t$, α, β, γ and k are arbitrary constants.

Set04: When $a_0 = -\frac{2\beta}{\gamma}$, $a_1 = 0$, $a_2 = \frac{3\beta}{\gamma}$, $b_1 = 0$, $b_2 = -\frac{3\beta}{\gamma}$, $\omega = \sqrt{\alpha^2 k^2 + \beta}$, the solutions become

$$H_7(\xi) = -\frac{2\beta}{\gamma} \pm i \left(-\frac{3\beta}{\gamma}\right) \tanh \xi \sec h \xi \pm \frac{3\beta}{\gamma} \tanh^2 \xi \quad (26)$$

and

$$H_8(\xi) = -\frac{2\beta}{\gamma} \pm \left(-\frac{3\beta}{\gamma}\right) \coth \xi \operatorname{csch} \xi \pm \frac{3\beta}{\gamma} \coth^2 \xi \quad (27)$$

where $\xi = kx - \sqrt{\alpha^2 k^2 + \beta}t$, and α, β, γ and k are free constants. The velocity of the wave solution Equations (24)–(27) is $\sqrt{\alpha^2 k^2 + \beta}/k$.

Set05: When $a_0 = \frac{3\beta}{\gamma}$, $a_1 = 0$, $a_2 = -\frac{3\beta}{\gamma}$, $b_1 = 0$, $b_2 = \frac{3\beta}{\gamma}$, $\omega = \sqrt{\alpha^2 k^2 - \beta}$, we achieve the solutions

$$H_9(\xi) = \frac{3\beta}{\gamma} \pm i \frac{3\beta}{\gamma} \tanh \xi \sec h \xi \pm \left(-\frac{3\beta}{\gamma}\right) \tanh^2 \xi \quad (28)$$

and

$$H_{10}(\xi) = \frac{3\beta}{\gamma} \pm \frac{3\beta}{\gamma} \coth \xi \operatorname{csch} \xi \pm \left(-\frac{3\beta}{\gamma}\right) \coth^2 \xi \tag{29}$$

where $\xi = kx - \sqrt{\alpha^2 k^2 - \beta}t$, and α, β, γ and k are arbitrary constants.

Set06: When $a_0 = \frac{3\beta}{\gamma}$, $a_1 = 0$, $a_2 = b_2 = -\frac{3\beta}{\gamma}$, $b_1 = 0$, $\omega = \sqrt{\alpha^2 k^2 - \beta}$, we derive the following solutions

$$H_{11}(\xi) = \frac{3\beta}{\gamma} \pm i \left(-\frac{3\beta}{\gamma}\right) \tanh \xi \operatorname{sech} \xi \pm \left(-\frac{3\beta}{\gamma}\right) \tanh^2 \xi \tag{30}$$

and

$$H_{12}(\xi) = \frac{3\beta}{\gamma} \pm \left(-\frac{3\beta}{\gamma}\right) \coth \xi \operatorname{csch} \xi \pm \left(-\frac{3\beta}{\gamma}\right) \coth^2 \xi \tag{31}$$

where $\xi = kx - \sqrt{\alpha^2 k^2 - \beta}t$, and α, β, γ and k are random constants. The velocity of the wave solutions Equations (28)–(31) is $\sqrt{\alpha^2 k^2 - \beta}/k$.

3.3. Multi-Soliton via Burgers' Equation

In this part, we derive the multi-soliton solution to the KGM via the Burger model as an auxiliary equation. The balance number of Equation (13) is $n = 2$, so the trial solution can be written as

$$H(\xi) = l_0 + l_1 B(\xi) + l_2 B^2(\xi). \tag{32}$$

Differentiating Equation (32) twice with the help of Equation (12) and setting these into Equation (13) yields a set of algebraic equations. Solving the sets for l_0, l_1, l_2 and ω_i yields

$$\text{Set01: } l_0 = 0, l_1 = \frac{6\beta}{\gamma \sum_{j=1}^n k_j}, l_2 = \frac{-6\beta}{\gamma \sum_{j=1}^n k_j^2}, \omega = \sqrt{\alpha^2 k^2 - \beta}$$

$$\text{Set02: } l_0 = \frac{\beta}{\gamma}, l_1 = \frac{-6\beta}{\gamma \sum_{j=1}^n k_j}, l_2 = \frac{6\beta}{\gamma \sum_{j=1}^n k_j^2}, \omega = \sqrt{\alpha^2 k^2 + \beta}$$

Utilizing **Set01** and **Set02** in the Equation (32) together with Equation (11), we achieve n -soliton solutions as follows:

$$U(x, t) = \frac{6\beta}{\gamma \sum_{j=1}^n k_j} \frac{\sum_{j=1}^n k_j e^{k_j x - \omega_j t}}{1 + \sum_{j=1}^n e^{k_j x - \omega_j t}} - \frac{6\beta}{\gamma \sum_{j=1}^n k_j} \left(\frac{\sum_{j=1}^n k_j e^{k_j x - \omega_j t}}{1 + \sum_{j=1}^n e^{k_j x - \omega_j t}} \right)^2, \omega_j = \sqrt{\alpha^2 k_j^2 - \beta}. \tag{33}$$

$$U(x, t) = \frac{\beta}{\gamma} - \frac{6\beta}{\gamma \sum_{j=1}^n k_j} \frac{\sum_{j=1}^n k_j e^{k_j x - \omega_j t}}{1 + \sum_{j=1}^n e^{k_j x - \omega_j t}} + \frac{6\beta}{\gamma \sum_{j=1}^n k_j} \left(\frac{\sum_{j=1}^n k_j e^{k_j x - \omega_j t}}{1 + \sum_{j=1}^n e^{k_j x - \omega_j t}} \right)^2, \omega_j = \sqrt{\alpha^2 k_j^2 + \beta}. \tag{34}$$

Remark 1. All of the obtained solutions were verified by returning them to Equation (1) with the computational software Maple and found to be correct. A numerical solver can compare their results with our obtained solutions.

4. Results and Discussions

In this part, we physically explain and discuss the features of the solutions of the quadratic nonlinear KGM via the GKM and the EShGE technique in 3-D graphics and contour plots.

4.1. Physical Descriptions for the Solutions of the KGM via the GKM

We present here dynamic properties, such as the rogue type, bright bell, and dark bell envelope, of the required solutions for the model via the KG scheme. Solution (15) demonstrates both solitonic and breather generation of rogue-type wave propagations for dissimilar conditions of the involved parameters. For the condition $\alpha^2 k^2 + \beta < 0$, the wave transformation presents as the intricate function, which is why the real and imaginary components of Equation (15) behaved as periodic rogue-type propagation. The profile and the particle density of the periodical rogue-form wave are demonstrated in Figure 1a (the real component) and Figure 1b (the imaginary component). Each rogue shape holds two elevation peaks and two deep humps, which are shown in the corresponding density plots under the 3D shapes. For the second condition, $\alpha^2 k^2 + \beta > 0$, solution (15) presents the real function and reveals the bell envelope soliton solution, and it displayed a bright bell-shape nature in favor of $\gamma > 0$ (Figure 1c), but a dark bell-shape nature with $\gamma < 0$ (Figure 1d).

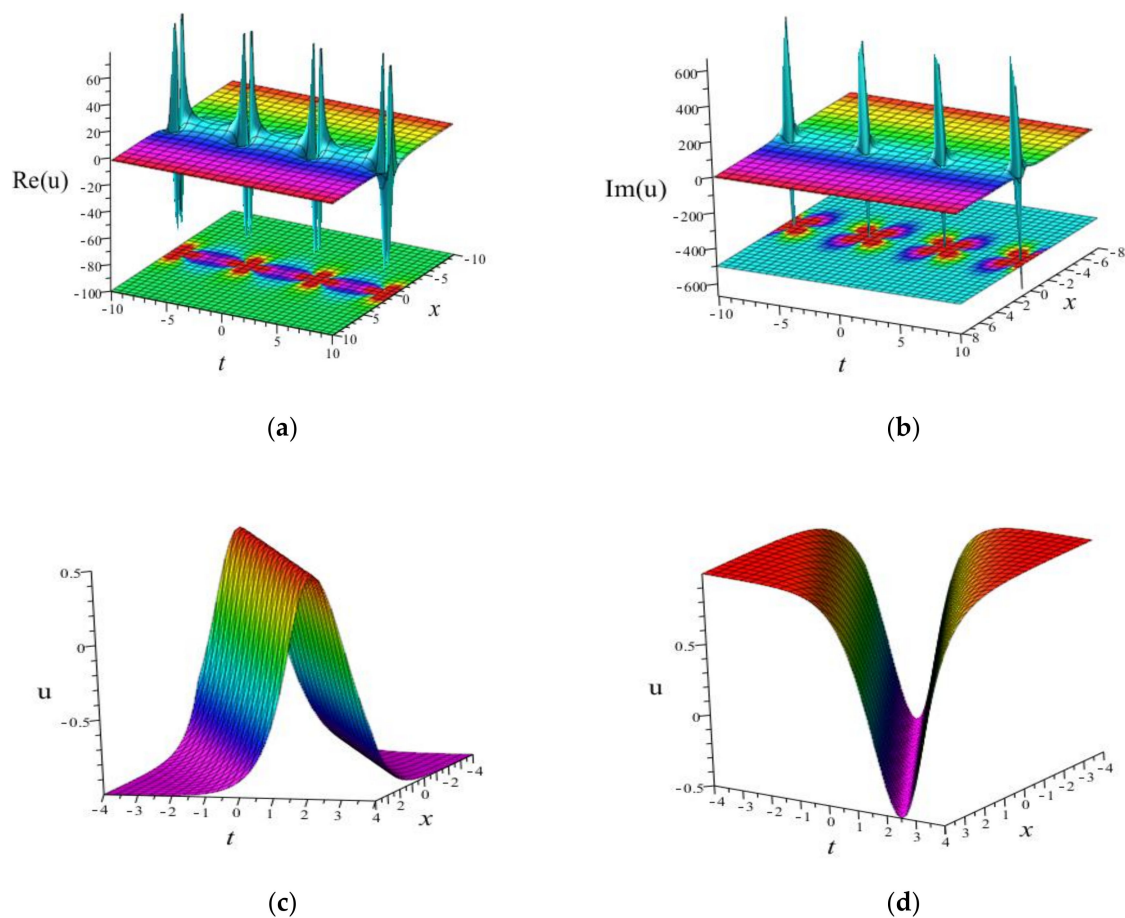


Figure 1. Four-petal rogue shape of Equation (15) for the values of parameters $\alpha = \gamma = h = b_0 = b_1 = k = 1, \beta = -2$: (a) real part of (15), whose 3D plot is above and density plot is below, (b) imaginary part of (9), whose 3D plot is above and density plot is below. Bell soliton solution (15) for the values of the parameters $\alpha = 1.25, h = b_0 = b_1 = k = \beta = 1$: (c) Bell-shape bright wave amid $\gamma = 1 > 0$, (d) Bell-shape dark wave amid $\gamma = -1 < 0$.

Solution (16) demonstrated solitonic as well as periodical rogue waves due to the distinct conditions of involved parameters. Under the condition $\alpha^2 k^2 - \beta < 0$, the propagation transformation presented the intricate function, and each component in Equation (16) behaved by the way of periodical rogue-type propagation (See Figure 2a: real part, Figure 2b: imaginary part). This is different from Figure 1a,b, as each rogue held three height cusp peaks and two deep humps that are shown in their corresponding density plots under the 3D shapes (see the density plot in Figure 2a,b). Again, for the condition $\alpha^2 k^2 - \beta > 0$,

solution (16) presents the real-valued function and exhibits a kink soliton (shock wave) solution bright for $\gamma > 0$ (Figure 2c) and dark for $\gamma < 0$ (Figure 2d).

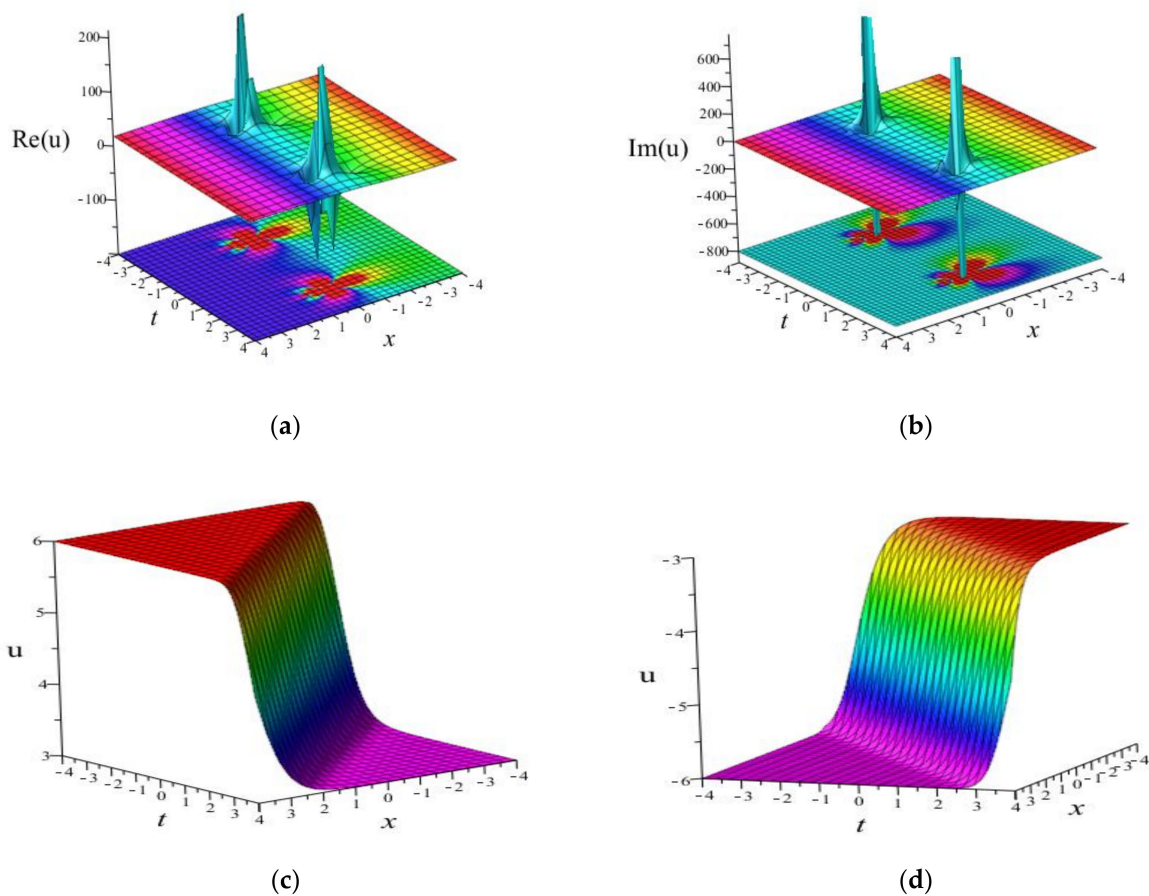


Figure 2. Four-petal rogue shape of Equation (16) for the values of the parameters $\alpha = \gamma = h = b_0 = b_1 = k = 1, \beta = 3$: (a) Real part of (16), whose 3D plot is above and density plot is below, (b) imaginary part of (16): 3D profile is above and density profile is below. Topological kink soliton solution (16) for the values of the parameters $\alpha = 1.25, \gamma = h = b_0 = b_1 = \beta = 1, k = 2$: (c) Bright kink soliton with $\gamma = 1 > 0$, (d) dark kink soliton with $\gamma = -1 < 0$.

The other solutions (17) and (18) both exhibit solitonic and periodic rogue waves, which were similar to (15). Solution (17) represented a rogue wave for $\omega^2 - \beta < 0$ and bell wave for $\omega^2 - \beta > 0$, which was bright for $\gamma > 0$ and dark for $\gamma < 0$. Solution (18) represents a rogue wave for $\omega^2 + \beta < 0$ and bell wave for $\omega^2 + \beta > 0$, which was bright for $\gamma > 0$ and dark for $\gamma < 0$. Since the natures of the other solutions were identical to Figure 1a–d, we ignored them for convenience.

4.2. Physical Descriptions for the Solutions of the KGM via the EShGE Technique

We present here the dynamic properties, such as the rogue shape, bright bell, and dark bell-shaped solitons of the required resolutions for the model via the EShGE scheme. Solutions (20) and (21) describe shock waves, and (21) and (23) exhibit singular solitons. All the solutions had solitonic as well as periodical rogue waves to apply, unlike the conditions of the existing parameters.

Solutions (20) and (21) represent rogue waves for $4\alpha^2k^2 - \beta < 0$, and bell waves for $4\alpha^2k^2 - \beta > 0$, which were bright for $\gamma > 0$ and dark for $\gamma < 0$. Solutions (22) and (23) represent rogue waves for $4\alpha^2k^2 + \beta < 0$, and bell waves for $4\alpha^2k^2 + \beta > 0$, which were bright for $\gamma > 0$ and dark for $\gamma < 0$. The natures of the other identical solutions were ignored as they had the same characteristics, similar to Figure 1a–d.

The other solutions (24), (26), (28), and (30) describe shock waves, and (25), (27), (29), and (31) exhibit singular solitons. All the solutions had solitonic as well as periodic rogue waves for dissimilar conditions of the involved parameters. Due to $\alpha^2 k^2 + \beta < 0$, the erratic transformation presented an intricate function, and a component of Equation (24) behaved as periodic rogue-type propagation. The profile and the particle density of the periodical rogue shapes are shown in Figure 3a (real component) and Figure 3b (imaginary component). Again for $\alpha^2 k^2 + \beta > 0$, solution (24) exhibited the bell-type soliton solution, whose real part exhibited a dark bell (see Figure 3c) and imaginary part exhibited a bright–dark nature (see Figure 3d) for $\gamma > 0$. However, for $\gamma < 0$, the real part exhibited only a bright bell (see Figure 3e) and the imaginary part behaved as dark–bright (see Figure 3f). As the profile of the other solutions was similar to that of Figure 3, we ignored them for convenience.

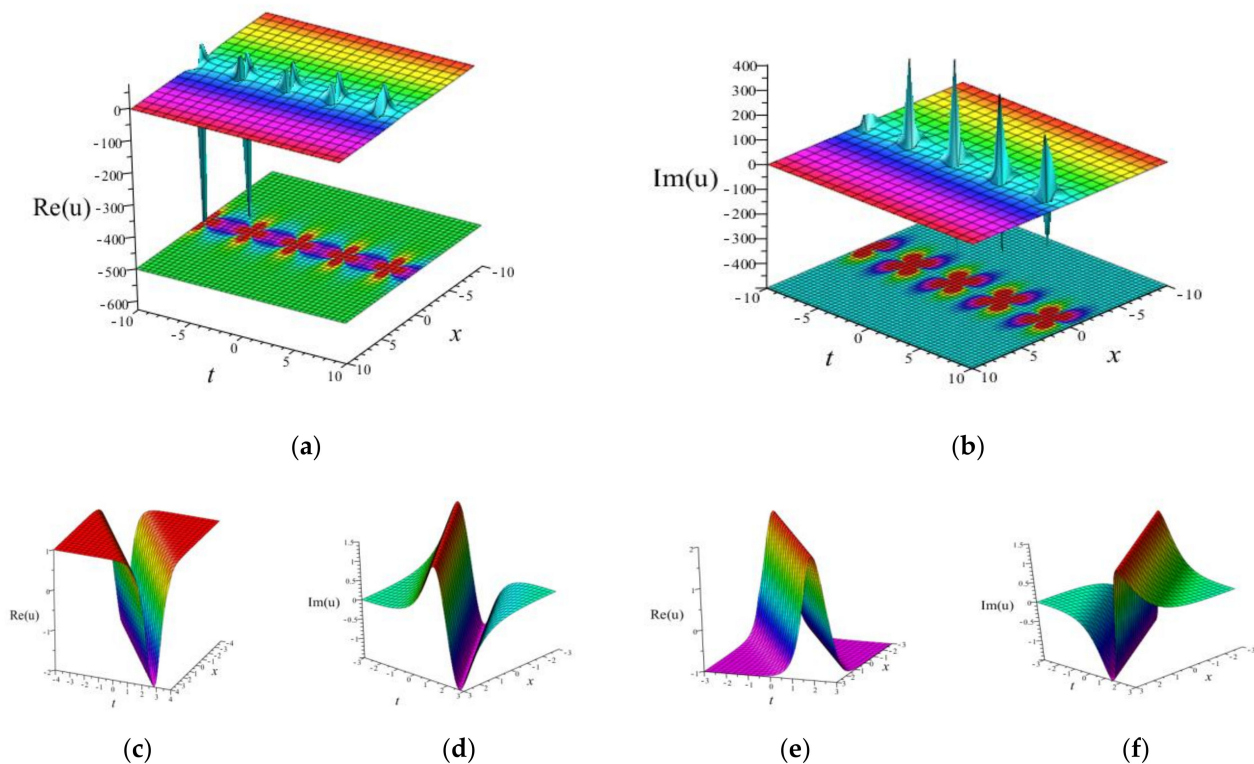


Figure 3. Four-petal rogue wave of solution (24) for the values $\alpha = k = \gamma = 1$, $\beta = -3$: (a) Real part of (24), whose 3D plot is above and density plot is below, (b) imaginary part of (24): 3D profile is above and density profile is below. Bell soliton solution (24) of the values $\alpha = k = \beta = 1$: (c) Real part of (24) with a dark bell wave, (d) imaginary part with a bright–dark bell wave with $\gamma = 1 > 0$. For $\gamma = -1 < 0$: (e) Real part of (24) with a bright bell wave, (f) imaginary part with a dark–bright bell wave.

4.3. Physical Descriptions for the Multi-Soliton Solutions of the KGM

We present here the dynamic-properties multi-soliton solution derived in Section 3.3. Both solutions (33) and (34) exhibited similar behaviors. For $n = 1, 2, 3, \dots, n$, provide one, two, three and so on upto n-solitons. In Figure 4, we present a few finite interactions of two and three solitons only. Here, we experience a non-elastic collision of solitons. Figure 4a shows that, before interaction ($t < 0$), there was only one kink, but after collision ($t > 0$), a single kink split into double kinks. Figure 4b shows that, before interaction ($t < 0$), there was a kink and a bell wave, but after collision ($t > 0$), it split into a double kink and a bell wave.

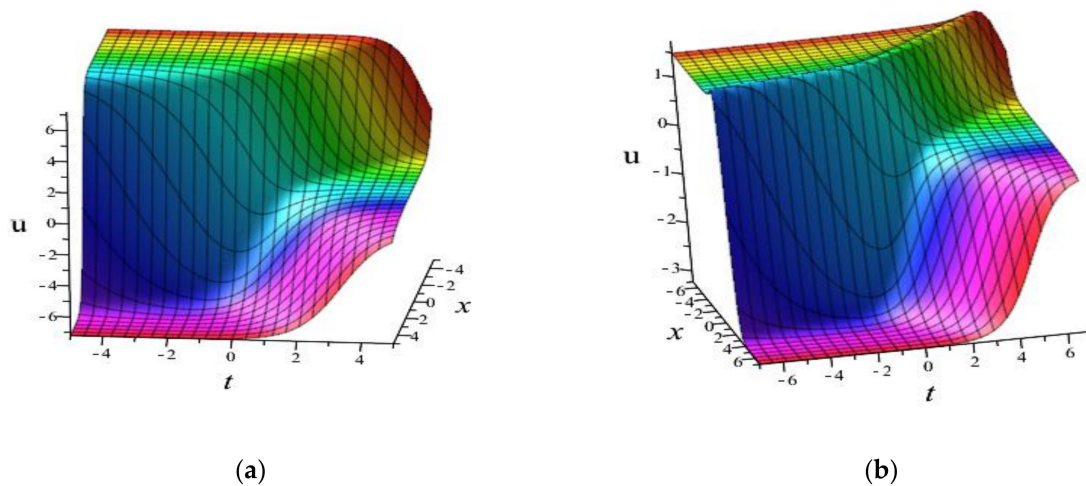


Figure 4. Four-petal rogue wave of solution (33) for the values $\alpha = k_1 = 1, \gamma = \beta = -1$: (a) Single kink splits into two kink waves for $k_2 = -2, n = 2$, (b) kink–bell soliton split into two kinks and a bell soliton for $n = 3, k_2 = -1.5, k_3 = -2$.

Remark 2. Anyone can see that the same solution reduces to another nature for the opposite sign of parametric conditions, which were discussed in the results and discussions section. The methods being performed with the help of a particular auxiliary equation is the limitation of our work.

5. Comparison

We observed that Agom and Ogunfeditimi [30] used a modified Adomian decomposition method to solve the quadratic nonlinear KGM and derived only periodic solutions. Additionally, Zhang [31] used the Exp-function method to solve the same KGM and found periodic and soliton solutions only. He had no parametric conditions and did not explain when, why, and which type of solitonic nature arose in his achieved solutions. In our investigation, we obtained bright-bell, dark-bell, and combined bright–dark bell-shaped solitons, combined dark–bright bell-shaped solitons, and periodic rogue-wave solutions. We use a different technique to derive a multi-soliton solution with the help of the Burger model and derived such non-elastic solitons, which were not found in previous literature with the auxiliary equation method. We also settled the parametric conditions for which one type of solitonic solution reduces to another type of solitonic nature in the previous section.

6. Conclusions

We successfully achieved a number of solitary envelope solutions of the quadratic nonlinear KGM in this manuscript. The results were obtained by means of reliable mathematical tools: the GKM and the EShGE technique. The methods play a substantial role in deriving exciting soliton solutions in terms of exponential functions. To apply different conditions to the existing parameters in the solutions, we constructed kink, anti-kink soliton, periodic rogue waves, bright bell, dark bell, combined bright–dark bell, combined dark–bright bell-shaped solitons, and multi-soliton solutions. The application of a few methods was restricted in obtaining periodic, kink, and bell soliton solutions in Refs. [30–34] only, but we acquired similar symmetric and non-symmetric periodic solitons, even a rogue-type breather wave solution, for this model via three schemes. We present and explain their natures in 3D profiles and contour plots. The importance of the dark, bright, and rogue soliton solutions has been clearly discussed in the literature [21–24] for the field of Bose–Einstein condensates only. Since the KGM (1) arises in different numerous scientific applications in relativistic quantum fields, such as the transmission of disruption and the Bloch wall activity of magnets in crystals, magnetic flux on a Josephson line, and a “splay wave” through a membrane, we think that our solutions can explain and be important for all such fields of KGM. The physical elucidation of the required solutions was described

with various adoptable parameters in quantum field theories. Moreover, the results and their graphical representations are highly interesting and applicable in solid-state physics and quantum field theories. Bifurcation analysis of the quadratic nonlinear KGM and the derivation of various types of solitary wave solutions according to each energy orbit of the phase portrait will be our next work. Numerical investigations of kinks carrying a charge [43], multi-kinks [44], and compact lumps [45] in higher fields from Lagrangian and direct experimental applications of obtained solutions in the mentioned fields will also be our future task.

Author Contributions: Methodology, Validation, and funding acquisition, A.A. (Alrazi Abdeljabbar); Conceptualization, Software, Writing—original draft, H.-O.R.; Supervision, Validation, and Data curation, A.A. (Abdullah Aldurayhim). All authors have read and agreed to the published version of the manuscript.

Funding: This research was funded by Khalifa University, Abu Dhabi, United Arab Emirates, and the APC will be funded by A. Abdeljabbar.

Institutional Review Board Statement: Not applicable.

Informed Consent Statement: Not applicable.

Acknowledgments: Thanks to editor, reviewers, and to Khalifa University, Abu Dhabi, United Arab Emirates, for financial support in this research.

Conflicts of Interest: The authors declare that they have no known competing financial interests or personal relationships that could have appeared to influence the work reported in this paper.

References

1. Kharif, C.; Pelinovsky, E.; Slunyaev, A. *Rogue Wave in the Ocean*; Springer: Berlin/Heidelberg, Germany, 2009.
2. Onorato, M.; Residori, S.; Bortolozzo, U.; Montina, A.; Arecchi, F.T. Rogue waves and their generating mechanisms in different physical contexts. *Phys. Rep.* **2013**, *528*, 47–89. [[CrossRef](#)]
3. Akhmediev, N.; Ankiewicz, A.; Taki, M. Waves that appear from nowhere and disappear without a trace. *Phys. Lett. A* **2009**, *373*, 675. [[CrossRef](#)]
4. Solli, D.R.; Repers, C.; Koonath, P.; Jalali, B. Optical rogue wave. *Nature* **2007**, *450*, 1054–1057. [[CrossRef](#)] [[PubMed](#)]
5. Bailung, H.; Sharma, S.K.; Nakamura, Y. Observation of Peregrine solitons in a multicomponent plasma with negative ions. *Phys. Rev. Lett.* **2011**, *107*, 255005. [[CrossRef](#)]
6. Sharma, S.K.; Bailung, H. Observation of hole Peregrine soliton in a multicomponent plasma with critical density of negative ions. *J. Geophys. Res. Space Phys.* **2013**, *118*, 919. [[CrossRef](#)]
7. Shats, M.; Punzmann, H.; Xia, H. Capillary Rogue waves. *Phys. Rev. Lett.* **2010**, *104*, 104503. [[CrossRef](#)] [[PubMed](#)]
8. Feng, L.L.; Zhang, T.T. Breather wave, rogue wave and solitary wave solutions of a coupled nonlinear Schrodinger equation. *Appl. Math. Lett.* **2018**, *78*, 133–140. [[CrossRef](#)]
9. Roshid, H.O.; Ma, W.X. Dynamics of mixed lump-solitary waves of an extended (2 + 1)-dimensional shallow water wave model. *Phys. Lett. A* **2018**, *382*, 3262–3268. [[CrossRef](#)]
10. Hossen, M.B.; Roshid, H.O.; Ali, M.Z. Characteristics of the solitary waves and rogue waves with interaction phenomena in a (2 + 1)-dimensional Breaking Soliton equation. *Phys. Lett. A* **2018**, *382*, 1268–1274. [[CrossRef](#)]
11. Atock, A.; Stéphane, N.W.; Augustin, D.; César, M.B. Extended (G'/G) Method Applied to the Modified Non-Linear Schrodinger Equation in the Case of Ocean Rogue Waves. *J. Mar. Sci.* **2014**, *4*, 246–256.
12. Yan, X.W.; Tian, S.F.; Dong, M.J.; Zou, L. Bäcklund transformation, rogue wave solutions and interaction phenomena for a (3 + 1)-dimensional B-type Kadomtsev–Petviashvili–Boussinesq equation. *Nonlinear Dyn.* **2018**, *92*, 709–720. [[CrossRef](#)]
13. Yang, B.; Chen, Y. General Rogue waves and their dynamics in several reverse time integrable nonlocal nonlinear equations. *arXiv* **2017**, arXiv:1712.05974.
14. Xu, S.; He, J. The rogue wave and breather solution of the Gerdjikov-Ivanov equation. *J. Math. Phys.* **2012**, *53*, 63507. [[CrossRef](#)]
15. Yue, Y.; Huang, L.; Chen, Y. N-solitons, breathers, lumps and rogue wave solutions to a (3 + 1)-dimensional nonlinear evolution equation. *Comput. Math. Appl.* **2017**, *75*, 2538–2548. [[CrossRef](#)]
16. Sulaiman, T.; Yusuf, A.; Abdeljabbar, A.; Alquran, M. Dynamics of lump collision phenomena to the (3 + 1)-dimensional nonlinear evolution equation. *J. Geom. Phys.* **2021**, *169*, 104347. [[CrossRef](#)]
17. Bazeia, D.; Losano, L. Deformed defects. *Phys. Rev. D* **2002**, *66*, 101701. [[CrossRef](#)]
18. Blinov, P.A.; Gani, T.V.; Gani, V.A. Deformations of kink tails. *Ann. Phys.* **2022**, *437*, 168739. [[CrossRef](#)]
19. Almeida, C.A.; Bazeia, D.; Losano, L.; Malbouisson, J.M.C. New results for deformed defects. *Phys. Rev. D* **2004**, *69*, 67702. [[CrossRef](#)]

20. Bazeia, D.; Belendryasova, E.; Gani, V.A. Scattering of kinks of the sinh-deformed ϕ^4 model. *Eur. Phys. J. C* **2018**, *78*, 340. [[CrossRef](#)]
21. Liang, Z.X.; Zhang, Z.D.; Liu, W.M. Dynamics of a bright soliton in Bose-Einstein condensates with time-dependent atomic scattering length in an expulsive parabolic potential. *Phys. Rev. Lett.* **2005**, *94*, 50402. [[CrossRef](#)]
22. Ji, A.C.; Liu, W.M.; Song, J.L.; Zhou, F. Dynamical creation of fractionalized vortices and vortex lattices. *Phys. Rev. Lett.* **2008**, *101*, 10402. [[CrossRef](#)] [[PubMed](#)]
23. Li, L.; Li, Z.; Malomed, B.A.; Mihalache, D.; Liu, W.M. Exact soliton solutions and nonlinear modulation instability in spinor Bose-Einstein condensates. *Phys. Rev. A* **2005**, *72*, 33611. [[CrossRef](#)]
24. Wang, D.S.; Hu, X.H.; Hu, J.P.; Liu, W.M. Quantized quasi-two-dimensional Bose-Einstein condensates with spatially modulated nonlinearity. *Phys. Rev. A* **2010**, *81*, 25604. [[CrossRef](#)]
25. Abdeljabbar, A. New double Wronskian solutions for a generalized (2 + 1)-dimensional Boussinesq system with variable coefficients. *Partial. Differ. Equ. Appl. Math.* **2021**, *3*, 100022. [[CrossRef](#)]
26. Abdeljabbar, A.; Tran, T.D. Pfaffian solutions to a generalized KP system with variable coefficients. *Appl. Math. Sci.* **2016**, *10*, 2351–2368. [[CrossRef](#)]
27. Kirane, M.; Abdeljabbar, A. Non-existence of global solutions of systems of time fractional Differential equations posed on the Heisenberg group. *Math. Methods Appl. Sci.* **2022**, *in press*.
28. Belendryasova, E.; Gani, V.A.; Zloshchastiev, K.G. Kink solutions in logarithmic scalar field theory: Excitation spectra, scattering, and decay of bions. *Phys. Lett. B* **2021**, *823*, 136776. [[CrossRef](#)]
29. Gani, V.A.; Marjaneh, A.M.; Javidan, K. Exotic final states in the ϕ^8 multi-kink collisions. *Eur. Phys. J. C* **2021**, *81*, 1124. [[CrossRef](#)]
30. Agom, E.U.; Ogunfiditimi, F.O. Exact solution of nonlinear Klein-Gordon equations with quadratic nonlinearity by Modified Adomian Decomposition method. *J. Math. Comput. Sci.* **2018**, *8*, 484–493.
31. Zhang, S. Exp-function method for Klein–Gordon equation with quadratic nonlinearity. *J. Phys.* **2008**, *96*, 12002. [[CrossRef](#)]
32. Xionghua, W.S. Numerical Solution of Klein-Gordon and sine-Gordon Equations using Chebyshev-Tau meshless Method. *Comput. Phys. Commun.* **2014**, *184*, 1399–1409.
33. Sirendaoreji. Auxiliary equation method and new solutions of Klein–Gordon equations. *Chaos Solitons Fractals* **2007**, *31*, 943–950. [[CrossRef](#)]
34. Roshid, H.O.; Rahman, N.; Akbar, M.A. Traveling waves solutions of nonlinear Klein Gordon equation by extended (G'/G)-expansion method. *Ann. Pure Appl. Math* **2013**, *2013*, 10–16.
35. Kudryashov, N.A. One method for finding exact solutions of nonlinear differential equations. *Commun. Nonlinear Sci. Numer. Simul.* **2012**, *17*, 2248–2253. [[CrossRef](#)]
36. Arnous, A.H.; Mirzazadeh, M. Application of the generalized Kudryashov method to the Eckhaus equation. *Nonlinear Anal. Model. Control.* **2017**, *21*, 577–586. [[CrossRef](#)]
37. Gaber, A.A.; Aljohani, A.F.; Ebaid, A.; Machado, J.T. The generalized Kudryashov method for nonlinear space–time fractional partial differential equations of Burgers type. *Nonlinear Dyn.* **2018**, *95*, 361–368. [[CrossRef](#)]
38. Islam, M.R.; Roshid, H.O. Application of generalized Kudryashov method to the Burger equation. *Int. J. Math. Trends Technol.* **2016**, *38*, 111–113. [[CrossRef](#)]
39. Yasar, E.; Yildirim, Y.; Adem, A.R. Perturbed optical solitons with spatio-temporal dispersion in (2 + 1)-dimensions by extended Kudryashov method. *Optik* **2018**, *158*, 1–14. [[CrossRef](#)]
40. Mahmud, F.; Samsuzzoha, M.; Akbar, M.A. The generalized Kudryashov method to obtain exact traveling wave solutions of the PHI-four equation and the Fisher equation. *Results Phys.* **2017**, *7*, 4296–4302. [[CrossRef](#)]
41. Ullah, M.S.; Roshid, H.O.; Ali, M.Z.; Rahman, Z. Novel exact solitary wave solutions for the time fractional generalized Hirota–Satsuma coupled KdV model through the generalized Kudryashov method. *Contemp. Math.* **2019**, *1*, 25–29.
42. Xian-Lin, X.; Jia-Shi, T. Travelling wave solutions for Konopelchenko–Dubrovsky equation using an extended sinh-Gordon equation expansion method. *Commun. Theor. Phys.* **2008**, *50*, 1047. [[CrossRef](#)]
43. Lensky, V.A.; Gani, V.A.; Kudryavtsev, A.E. Domain walls carrying a U(1) charge. *J. Exper. Theor. Phys.* **2001**, *93*, 677–684. [[CrossRef](#)]
44. Gani, V.A.; Marjaneh, A.M.; Blinov, P.A. Explicit kinks in higher-order field theories. *Phys. Rev. D* **2020**, *101*, 125017. [[CrossRef](#)]
45. Bazeia, D.; Marques, M.A.; Menezes, R. Compact lumps. *EPL* **2015**, *111*, 61002. [[CrossRef](#)]